

Supporting information

Twenty crystal structures of bromodomain and PHD finger containing protein 1 (BRPF1)/ligand complexes reveal conserved binding motifs and rare interactions

Jian Zhu and Amedeo Caflisch*

Department of Biochemistry, University of Zürich, Winterthurerstrasse 190, CH-8057 Zürich, Switzerland

*E-mail: caflisch@bioc.uzh.ch

Table of contents

Fig S1. Top ranked binding mode of fragments 1 , 2 , 3 and 8	1
Fig S2. False positive hits from fragment docking.	2
Fig S3. Plot of similarity matrix of compounds 1 to 16	3
BromoScan assay	4
Fig S4. Dose-response curves for compounds obtained using the competition binding assay at DiscoverX with BRPF1b.	5
Fig S5. IC ₅₀ value of compound 20 determined by AlphaScreen binding assay.....	6
Table S1. X-ray data collection and refinement statistics for complex structures with 1 , 2 , 3 and 4	7
Table S2. X-ray data collection and refinement statistics for complex structures with 5 , 6 , 7 and 8	8
Table S3. X-ray data collection and refinement statistics for complex structures with 9 , 10 , 11 and 12	9
Table S4. X-ray data collection and refinement statistics for complex structures with 13 , 14 , 15 and 16	10
Table S5. X-ray data collection and refinement statistics for complex structures with 18 , 19 , and 20	11
Fig S6. Close view of binding mode of compounds 1 , 2 , 3 , 4 , 5 and 6	12
Fig S7. Close view of binding mode of compounds 7 , 8 , 9 , 10 , 11 and 12	13
Fig S8. Close view of binding mode of compounds 13 , 14 , 15 , 16 , 17 , 18 , 19 and 20	14
Fig S9. Chemical structures of inhibitors for structural comparison.	15
Fig S10. Binding mode comparison of the dihydroquinolin ligands bound to bromodomain proteins.	16
Fig S11. Binding mode comparison of the 9H-purine ligands bound to bromodomain proteins.	17

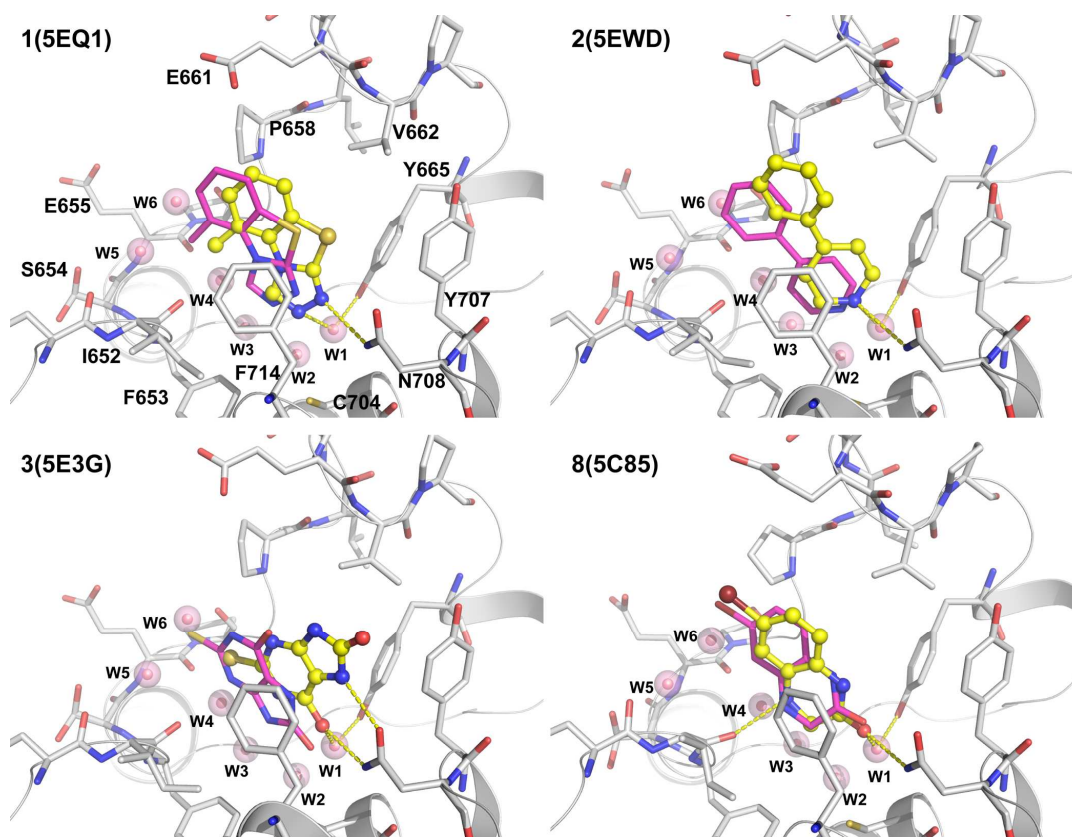


Fig S1. Comparison of docked pose obtained by the fragment-docking program SEED (carbon atoms in magenta) and binding mode in the crystal structure (carbon atoms in yellow) of fragments **1**, **2**, **3** and **8**. Heteroatoms are colored as follows: N (blue), O (red), S (yellow), and Br (maroon). The six conserved water molecules in the Kac binding pocket are labeled W1 to W6.

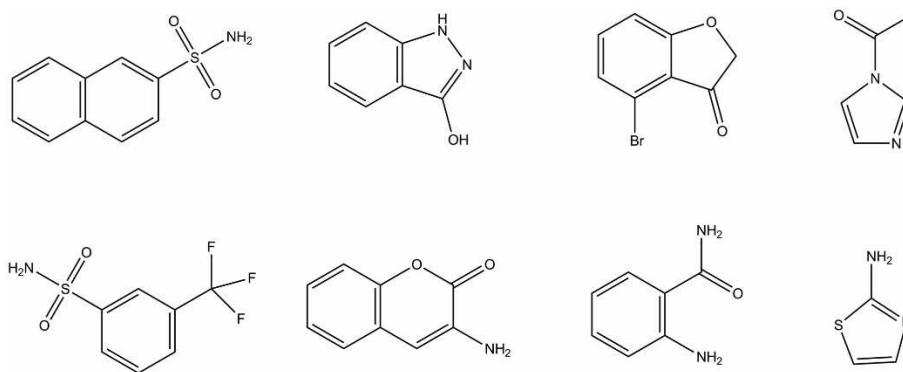


Fig S2. False positive hits from fragment docking by SEED. These fragments were among the 13 fragments purchased from 30 top ranked ones, but binding is not observed by X-ray crystallography (soaking into BRPF₁ apo crystals).

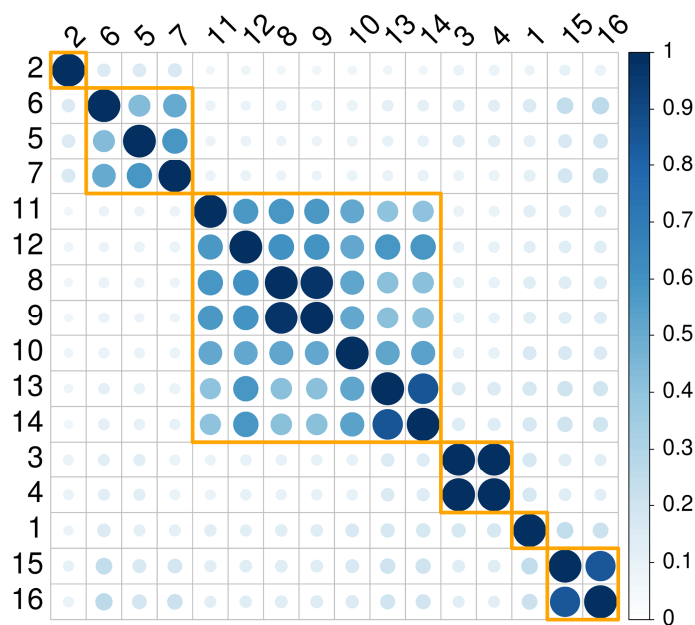


Fig S3. Similarity matrix of compounds **1** to **16**. The similarity (Tanimoto coefficient) was calculated based on the RDKit fingerprint which is implemented in the RDKit[†] toolkit. The size and darkness (vertical legend on the right) of the circles indicate similarity. The hierarchical complete-link algorithm with the R programming language generates six clusters (orange boxes).

BromoScan assay²

BromoScan assays on BRPF1 for the 14 compounds were performed at DiscoverX. T7 phage strains displaying bromodomains were grown in parallel in 24-well blocks in an *E. coli* host derived from the BL21 strain. *E. coli* were grown to log-phase and infected with T7 phage from a frozen stock (multiplicity of infection= 0.4) and incubated with shaking at 32°C until lysis (90-150 minutes). The lysates were centrifuged (5,000 x g) and filtered (0.2 µm) to remove cell debris. Streptavidin-coated magnetic beads were treated with biotinylated small molecule or acetylated peptide ligands for 30 minutes at room temperature to generate affinity resins for bromodomain assays. The liganded beads were blocked with excess biotin and washed with blocking buffer (SeaBlock (Pierce), 1 % BSA, 0.05 % Tween 20, 1 mM DTT) to remove unbound ligand and to reduce non-specific phage binding. Binding reactions were assembled by combining bromodomains, liganded affinity beads, and test compounds in 1x binding buffer (17% SeaBlock, 0.33x PBS, 0.04% Tween 20, 0.02% BSA, 0.004% Sodium azide, 7.4 mM DTT). Test compounds were prepared as 1000X stocks in 100% DMSO and subsequently diluted 1:10 in monoethylene glycol (MEG) to create stocks at 100X the screening concentration (resulting stock solution is 10% DMSO/90% MEG). The compounds were then diluted directly into the assays such that the final concentration of DMSO and MEG were 0.1% and 0.9%, respectively. All reactions were performed in polystyrene 96-well plates in a final volume of 0.135 ml.

The assay plates were incubated at room temperature with shaking for 1 hour and the affinity beads were washed with wash buffer (1x PBS, 0.05% Tween 20). The beads were then re-suspended in elution buffer (1x PBS, 0.05% Tween 20, 2 µM nonbiotinylated affinity ligand) and incubated at room temperature with shaking for 30 minutes. The bromodomain concentration in the eluates was measured by qPCR. Binding constants (Kds) were calculated with a standard dose-response curve using the Hill equation:

$$\text{Response} = \text{Background} + \frac{\text{Signal} - \text{Background}}{1 + (K_d^{\text{Hill Slope}} / \text{Dose}^{\text{Hill Slope}})}$$

Curves were fitted using a non-linear least square fit with the Levenberg-Marquardt algorithm.

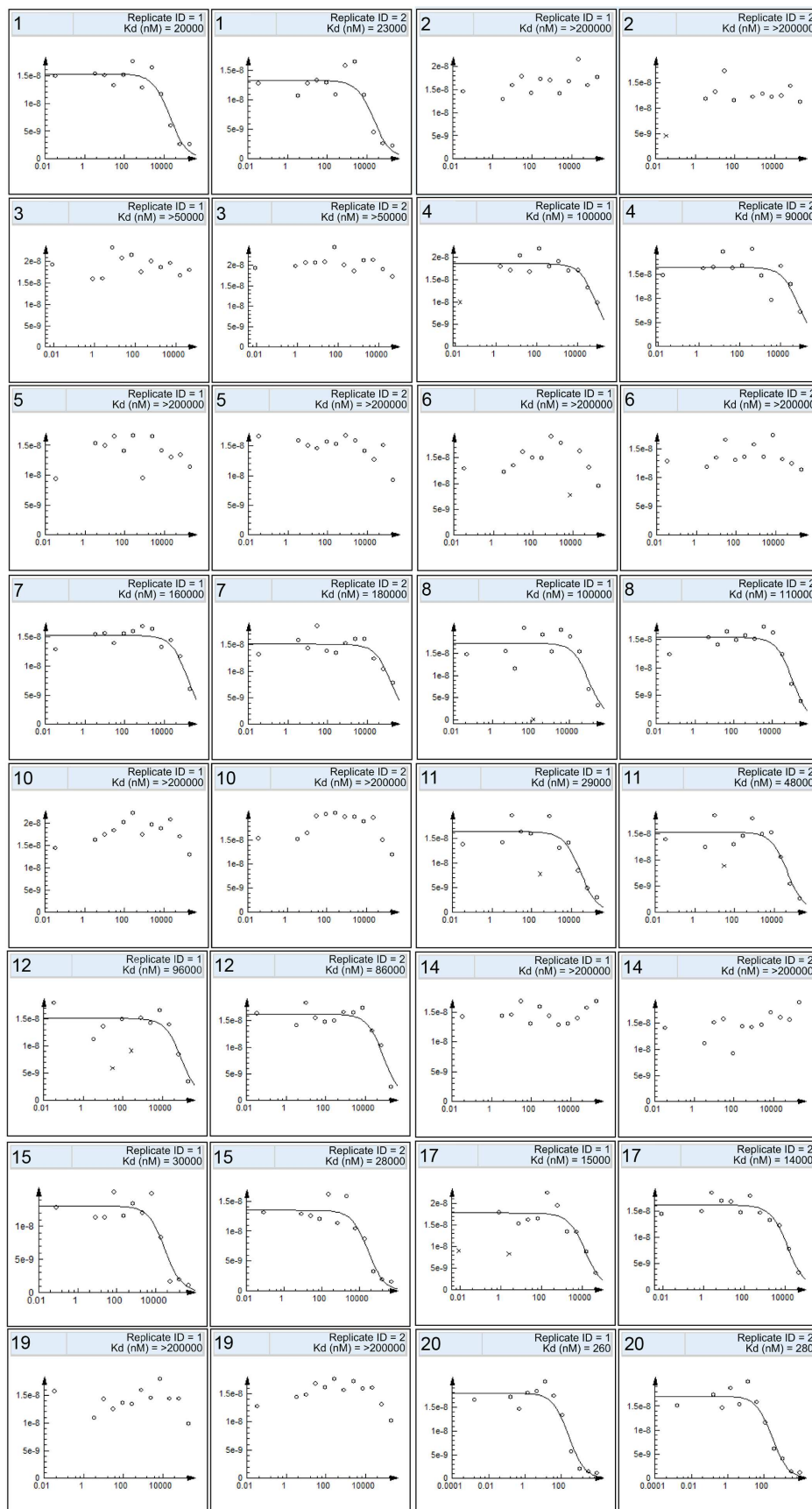


Fig S4. Dose-response curves in duplicates for the 16 compounds tested for binding to the BRPF1 bromodomain in the competition binding assay at DiscoverX.

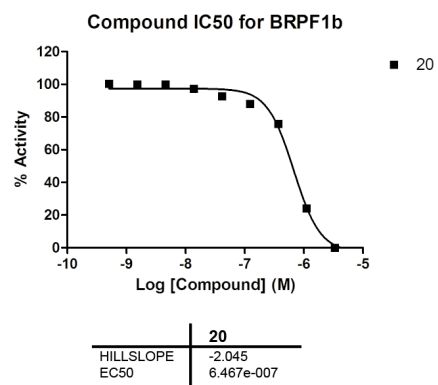


Fig S5. IC₅₀ value of compound **20** determined by the AlphaScreen binding assay³ at Reaction Biology.

Table S1. X-ray data collection and refinement statistics for complex structures of the BRPF1 bromodomain and compounds **1**, **2**, **3** and **4**.

Data Collection				
PDB ID	5EQ1	5EWD	5E3G	5E3D
ligand	1	2	3	4
space group	P ₃ ₂ ₁	P ₃ ₂ ₁	P ₃ ₂ ₁	P ₃ ₂ ₁
Cell dimensions				
a, b, c (Å)	60.38, 60.38, 63.20	60.67, 60.67, 63.02	60.86, 60.86, 62.99	60.73, 60.73, 62.43
α, β, γ (°)	90.00, 90.00, 120.00	90.00, 90.00, 120.00	90.00, 90.00, 120.00	90.00, 90.00, 120.00
resolution (Å)	40.29 - 1.55	40.36 - 1.58	40.40 - 1.65	40.22 - 1.71
unique observations*	19761(2835)	18839(2686)	16662(2374)	14799(2108)
completeness*	99.9 (100.0)	100.0(100.0)	100.0(100.0)	99.7(99.1)
redundancy*	9.4 (8.9)	9.6(9.6)	9.7(10.0)	9.5(9.6)
Rmerge*	0.041 (0.338)	0.029(0.359)	0.040(0.442)	0.031(0.405)
I/σI*	25.9 (6.1)	34.7(5.7)	25.6(4.9)	30.3(5.1)
Refinement				
R _{work} /R _{free} *	0.189(0.229)/0.194(0.292)	0.199(0.233)/0.225(0.252)	0.196(0.208)/0.205(0.268)	0.192(0.241)/0.222(0.319)
r.m.s deviations of bond lengths (Å)	0.008	0.006	0.007	0.007
r.m.s deviations of bond angles (°)	0.879	0.666	0.765	0.710
no. of non-hydrogen atom / average B-factor (Å ²)				
protein	946/37.56	946/40.90	944/45.24	936/48.64
ligand	13/40.53	12/56.25	12/57.45	12/59.34
water	80/43.30	103/46.65	64/46.49	75/48.63
residues in protein chain	628 - 739	627 - 739	628 - 739	628 - 739
Ramachandran				
Favored	98.25	100.00	99.12	99.12
allowed	1.75	0.00	0.88	0.88
disallowed	0.00	0.00	0.00	0.00
* Highest resolution shell is shown in parentheses.				

Table S2. X-ray data collection and refinement statistics for complex structures of the BRPF₁ bromodomain and compounds **5**, **6**, **7** and **8**.

Data Collection				
PDB ID	5C87	5EM3	5EWH	5C85
ligand	5	6	7	8
space group	P ₃ ₂ ₁	P ₃ ₂ ₁	P ₃ ₂ ₁	P ₃ ₂ ₁
Cell dimensions				
a, b, c (Å)	60.56, 60.56, 63.60	60.14, 60.14, 63.23	60.44, 60.44, 62.68	60.72, 60.72, 61.87
α, β, γ (°)	90.00, 90.00, 120.00	90.00, 90.00, 120.00	90.00, 90.00, 120.00	90.00, 90.00, 120.00
resolution (Å)	30.00 - 1.55	40.20 - 1.40	40.18 - 1.63	40.07 - 1.70
unique observations*	20025(2861)	26409(3814)	16966(2453)	14925(2129)
completeness*	100.0(100.0)	99.7(99.7)	100.0(100.0)	100.0(100.0)
redundancy*	9.1(6.0)	9.2(8.8)	9.5(9.9)	9.7(9.5)
Rmerge*	0.048(0.341)	0.049(0.236)	0.073(0.358)	0.031(0.326)
I/σI*	26.6(4.8)	25.4(8.4)	16.3(5.3)	37.1(6.5)
Refinement				
Rwork/Rfree*	0.181(0.221)/0.198(0.26)	0.173(0.187)/0.196(0.224)	0.190(0.212)/0.223(0.288)	0.207(0.241)/0.225(0.269)
r.m.s deviations of bond lengths (Å)	0.007	0.010	0.006	0.007
r.m.s deviations of bond angles (°)	0.920	0.780	0.743	0.931
no. of non-hydrogen atom / average B-factor (Å ²)				
protein	947/38.01	974/19.79	955/28.65	929/50.59
ligand	11/44.55	22/22.39	11/40.01	12/55.99
water	124/44.19	170/30.45	134/40.01	79/48.55
residues in protein chain	628 - 739	625 - 739 (extra serine residue 625 at the N terminal)	627 - 739	628 -739
Ramachandran				
Favored	99.12	99.15	99.14	99.12
allowed	0.88	0.85	0.86	0.88
disallowed	0.00	0.00	0.00	0.00
* Highest resolution shell is shown in parentheses.				

Table S3. X-ray data collection and refinement statistics for complex structures of the BRPF₁ bromodomain and compounds **9**, **10**, **11** and **12**.

Data Collection				
PDB ID	5DYC	5DY7	5EPS	5EPR
ligand	9	10	11	12
space group	P ₃ ₂ ₁	P ₃ ₂ ₁	P ₃ ₂ ₁	P ₃ ₂ ₁
Cell dimensions				
a, b, c (Å)	60.81, 60.81, 63.11	60.67, 60.67, 62.38	60.63, 60.63, 62.50	60.92, 60.92, 63.02
α, β, γ (°)	90.00, 90.00, 120.00	90.00, 90.00, 120.00	90.00, 90.00, 120.00	90.00, 90.00, 120.00
resolution (Å)	40.44 - 1.65	40.19 - 1.69	40.20 - 1.47	40.45 - 1.65
unique observations*	16556(2353)	15153(2094)	23061(3316)	16718(2400)
completeness*	99.5(99.3)	99.2(95.5)	100.0(99.8)	100.0(100.0)
redundancy*	9.7(10.0)	9.5(9.3)	9.5(9.3)	9.5(9.9)
Rmerge*	0.039(0.408)	0.060(0.440)	0.042(0.285)	0.035(0.366)
I/σI*	28.2(5.4)	18.7(4.5)	25.4(6.6)	28.6(5.6)
Refinement				
Rwork/Rfree*	0.198(0.237)/0.235(0.289)	0.179(0.243)/0.204(0.306)	0.188(0.202)/0.198(0.250)	0.198(0.264)/0.220(0.285)
r.m.s deviations of bond lengths (Å)	0.006	0.007	0.007	0.008
r.m.s deviations of bond angles (°)	0.694	0.773	0.738	0.681
no. of non-hydrogen atom / average B-factor				
protein	951/43.43	956/31.17	952/32.75	948/44.14
ligand	12/53.58	15/39.11	12/47.99	12/59.44
water	82/46.97	142/37.17	111/39.47	71/45.87
residues in protein chain	627 - 739	627 - 739	627 - 739	628 - 739
Ramachandran(%)				
Favored	99.13	99.15	100.00	99.12
allowed	0.87	0.85	0.00	0.88
disallowed	0.00	0.00	0.00	0.00
* Highest resolution shell is shown in parentheses.				

Table S4. X-ray data collection and refinement statistics for complex structures of the BRPF₁ bromodomain and compounds **13**, **14**, **15** and **16**.

Data Collection				
PDB ID	5EWC	5DYA	5ETB	5ETD
ligand	13	14	15	16
space group	P ₃ ₂ 21	P ₃ ₂ 21	P ₃ ₂ 21	P ₃ ₂ 21
Cell dimensions				
a, b, c (Å)	60.93, 60.93, 63.05	61.16, 61.16, 62.15	60.37, 60.37, 63.50	60.32, 60.32, 62.92
α, β, γ (°)	90.00, 90.00, 120.00	90.00, 90.00, 120.00	90.00, 90.00, 120.00	90.00, 90.00, 120.00
resolution (Å)	40.46 - 1.75	40.31 - 1.65	40.36 - 1.33	40.19 - 1.40
unique observations*	14043(1999)	16557(2370)	31032(4300)	26520(3791)
completeness*	100.0(99.9)	99.8(100.0)	99.3(95.6)	99.9(99.5)
redundancy*	9.7(9.7)	9.5(9.8)	8.7(4.9)	9.2(8.4)
Rmerge*	0.049(0.406)	0.027(0.417)	0.038(0.158)	0.044(0.334)
I/σI*	24.1(5.1)	37.1(5.2)	31.1(7.8)	22.9(5.3)
Refinement				
Rwork/Rfree*	0.194(0.252)/0.211(0.312)	0.186(0.214)/0.213(0.264)	0.174(0.204)/0.186(0.235)	0.176(0.215)/0.186(0.219)
r.m.s deviations of bond lengths (Å)	0.008	0.007	0.008	0.008
r.m.s deviations of bond angles (°)	0.731	0.790	0.791	0.756
no. of non-hydrogen atom / average B-factor				
protein	942/46.33	937/39.08	944/21.15	944/25.24
ligand	17/58.74	16/52.93	13/26.45	12/27.97
water	91/49.34	115/43.46	179/34.57	138/34.71
residues in protein chain	628 - 739	628 - 739	628 - 739	628 - 739
Ramachandran				
Favored	99.12	99.12	98.23	99.12
allowed	0.88	0.88	1.77	0.88
disallowed	0.00	0.00	0.00	0.00
* Highest resolution shell is shown in parentheses.				

Table S5. X-ray data collection and refinement statistics for complex structures of the BRPF₁ bromodomain and compounds **18**, **19**, and **20**.

Data Collection			
PDB ID	5EV9	5EVA	5C7N
ligand	18	19	20
space group	P ₃ ₂ ₁	P ₃ ₂ ₁	P ₃ ₂ ₁
Cell dimensions			
a, b, c (Å)	60.36, 60.36, 63.46	60.36, 60.36, 63.39	60.50, 60.50, 63.11
α, β, γ (°)	90.00, 90.00, 120.00	90.00, 90.00, 120.00	90.00, 90.00, 120.00
resolution (Å)	40.35 - 1.45	40.33 - 1.45	40.31 - 1.75
unique observations*	24170(3476)	24128(3476)	13890(1986)
completeness*	100.0(99.9)	99.9(100.0)	100.0(100.0)
redundancy*	9.4(9.3)	9.3(9.0)	9.7(9.8)
Rmerge*	0.032(0.285)	0.041(0.292)	0.044(0.420)
I/σI*	33.0(6.9)	27.6(7.0)	27.5(5.4)
Refinement			
Rwork/Rfree*	0.188(0.242)/0.221(0.257)	0.183(0.222)/0.197(0.235)	0.180(0.229)/0.220(0.289)
r.m.s deviations of bond angles (°)	0.009	0.008	0.010
r.m.s deviations of bond lengths (Å)	0.885	0.834	0.987
no. of non-hydrogen atom / average B-factor			
protein	939/38.50	938/32.67	955/45.50
ligand	19/50.15	17/46.97	28/62.80
water	130/46.12	152/42.00	102/48.89
residues in protein chain	628 - 739	627 - 739	628 - 739
Ramachandran			
Favored	99.12	98.23	97.39
allowed	0.88	1.77	2.61
disallowed	0.00	0.00	0.00
* Highest resolution shell is shown in parentheses.			

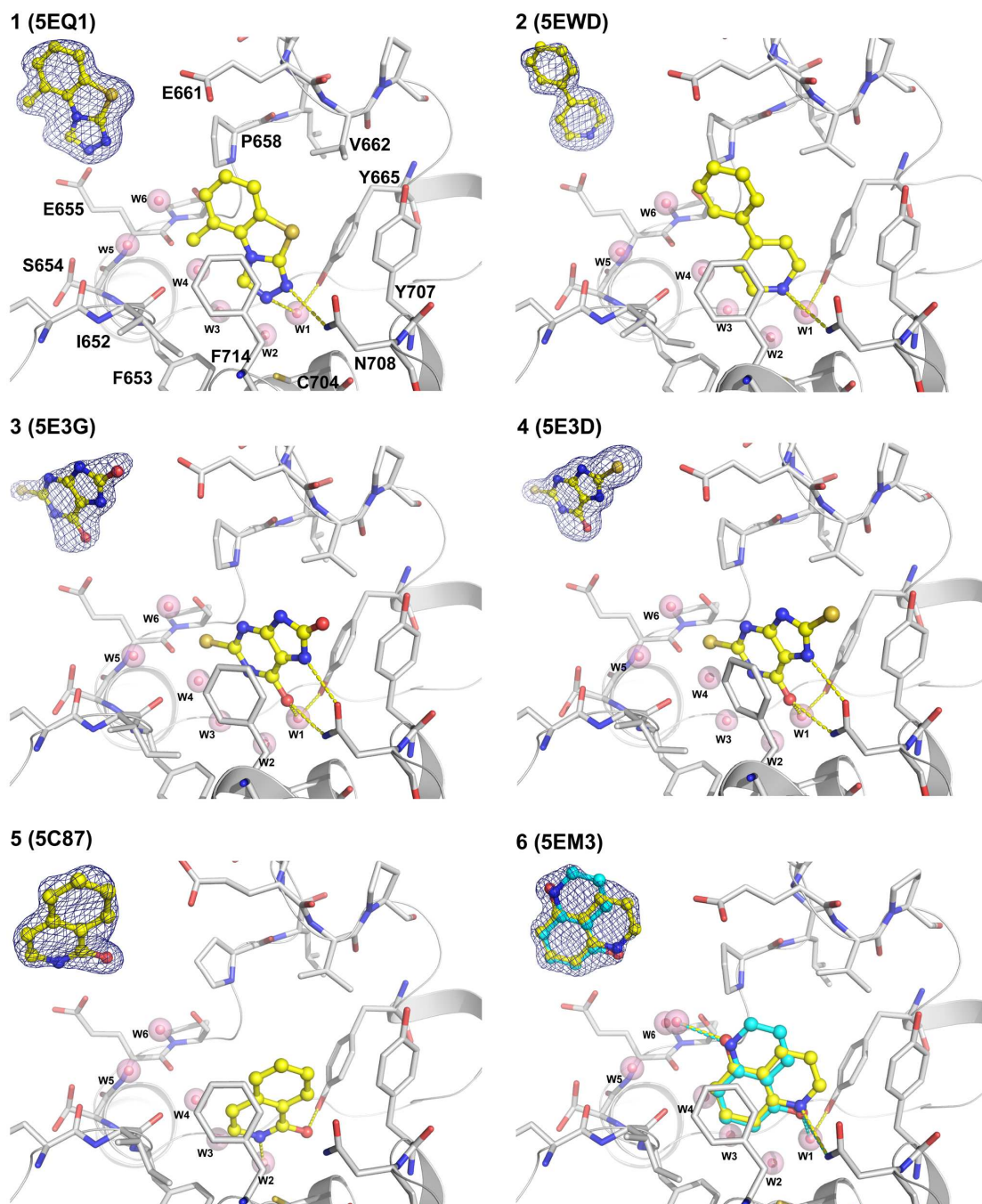


Fig S6. Close view of binding mode of compounds **1**, **2**, **3**, **4**, **5** and **6**. Conserved water molecules in the binding pocket are labeled W1 to W6 (pink spheres). $2F_o-F_c$ electron density maps contoured at 1σ for ligands are shown by a mesh. Two alternative conformations of fragment **6** are shown in yellow and cyan.

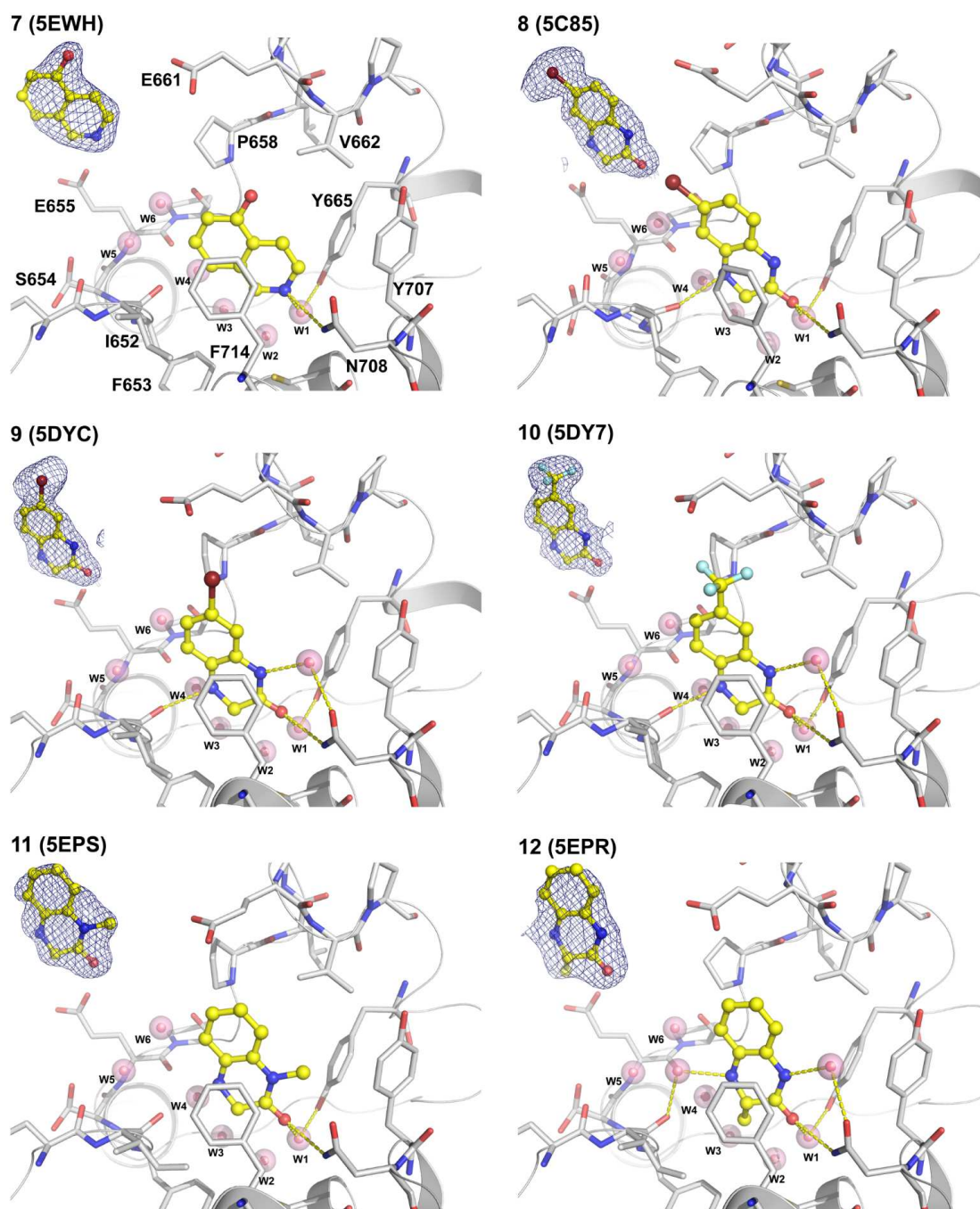


Fig S7. Same as Figure S7 for compounds **7**, **8**, **9**, **10**, **11** and **12**. For fragments **7** and **12**, $2F_o-F_c$ electron density maps are contoured at 0.8σ .

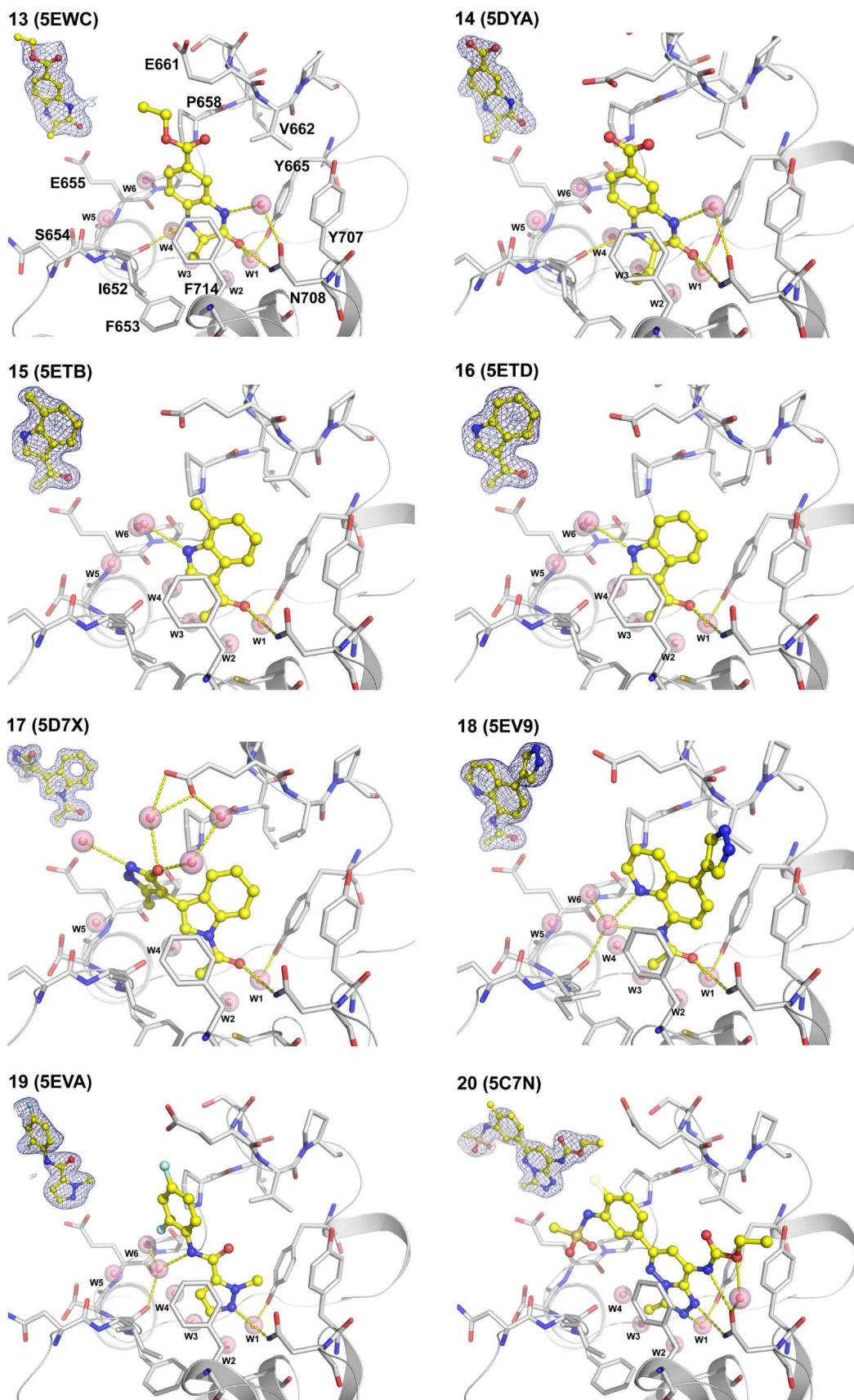


Fig S8. Same as Figure S7 for compounds 13, 14, 15, 16, 17, 18, 19 and 20. For ligands 19 and 20, 2Fo-Fc electron density maps are contoured at 0.8σ .

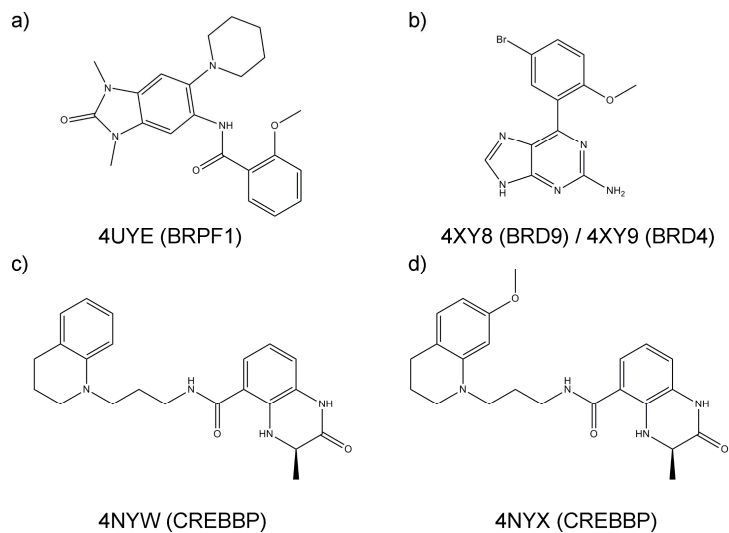


Fig S9. Chemical structures of inhibitors for structural comparison.

(a) N-[1,3-dimethyl-2-oxo-6-(piperidin-1-yl)-2,3-dihydro-1H-benzimidazol-5-yl]-2-methoxybenzamide, (b) 6-(5-bromo-2-methoxyphenyl)-9H-purin-2-amine, (c) (3R)-N-[3-(3,4-dihydroquinolin-1(2H)-yl)propyl]-3-methyl-2-oxo-1,2,3,4-tetrahydroquinoxaline-5-carboxamide, and (d) (3R)-N-[3-(7-methoxy-3,4-dihydroquinolin-1(2H)-yl)propyl]-3-methyl-2-oxo-1,2,3,4-tetrahydroquinoxaline-5-carboxamide.

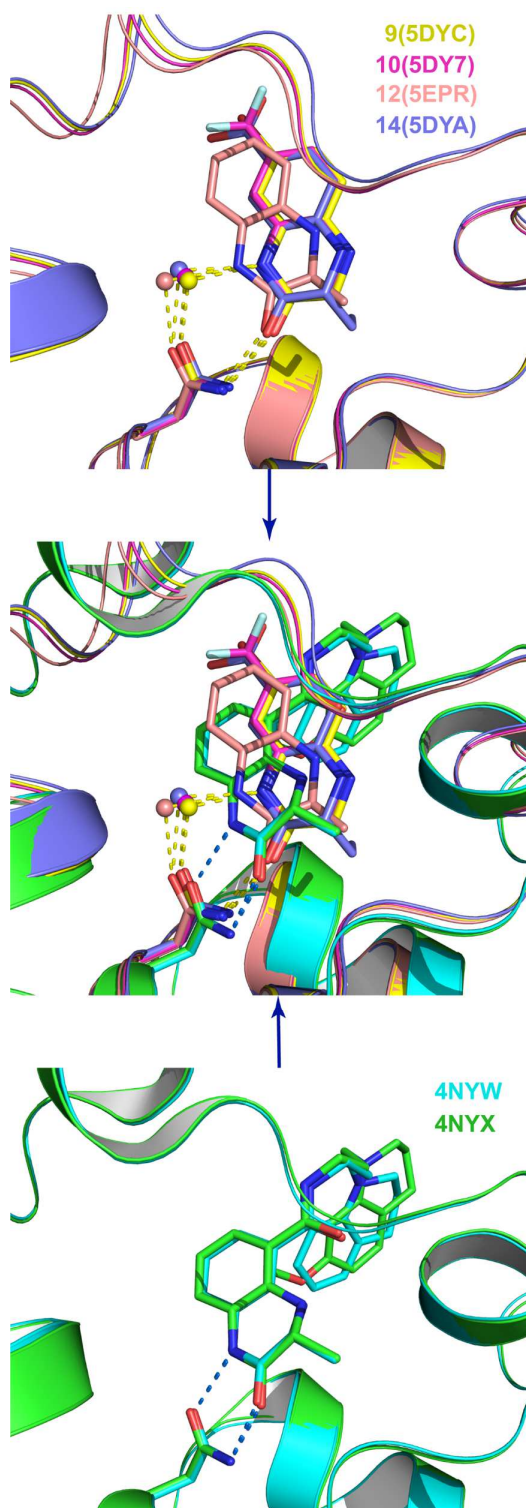


Fig S10. Comparison of the binding modes of dihydroquinoline ligands in BRPF1 (top) and CREBBP (bottom). The structural alignment (middle) shows that the binding modes are different. (Top) In BRPF1, the bromine substituent of fragment **9**, the trifluoromethyl of **10**, and the carboxylate of **14** occupy the same position, while fragment **12** (5EPR) is devoid of substituent and its orientation is slightly shifted.

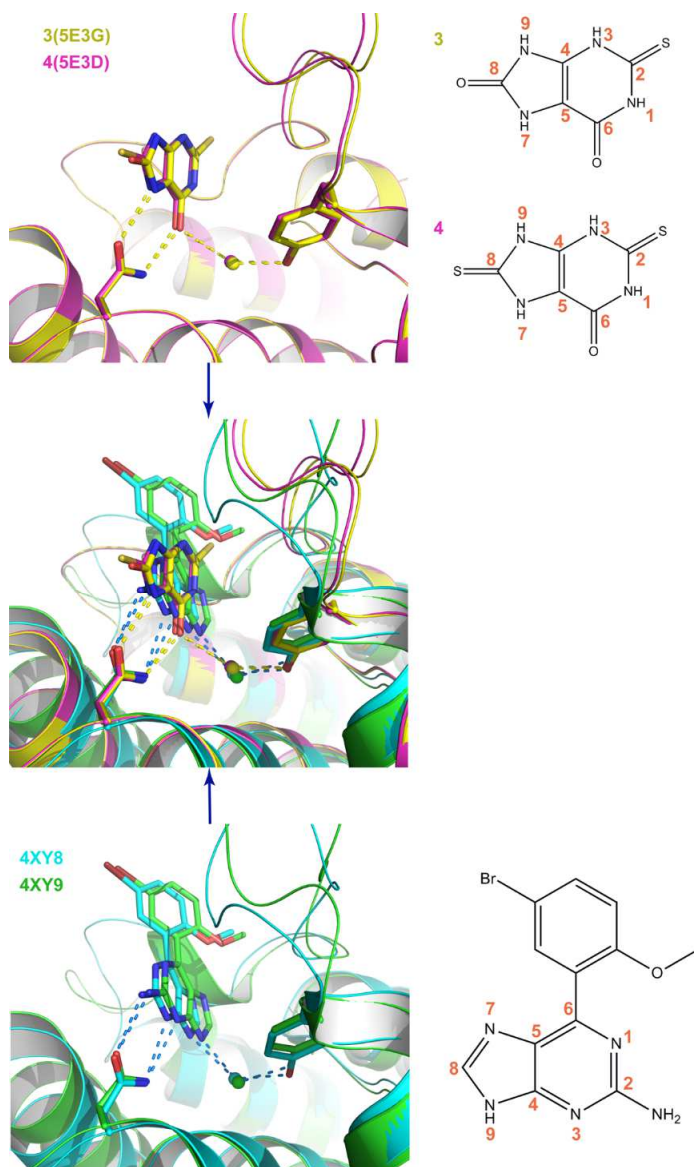


Fig S11. Comparison of the binding modes of mercaptopurine fragments **3** and **4** in BRPF1 (top) with the previously reported 2-amine-9H-purine ligands of the BRD9 (**4XY8**, bottom) and BRD4 (**4XY9**, bottom) bromodomains. The structural alignment (middle) shows that the binding modes are different which is consistent with the fact that these ligands share only the purine scaffold.

Reference

1. RDKit: cheminformatics and machine learning software. **2013**. <http://www.rdkit.org> (accessed January 3, 2016).
2. Quinn, E.; Wodicka, L.; Ciceri, P.; Pallares, G.; Pickle, E.; Torrey, A.; Floyd, M.; Hunt, J.; Treiber, D. Abstract 4238: BROMOScan - a high throughput, quantitative ligand binding platform identifies best-in-class bromodomain inhibitors from a screen of mature compounds targeting other protein classes *Cancer Res.* **2013**, *73*, 4238.
3. Philpott, M.; Yang, J.; Tumber, T.; Fedorov, O.; Uttarkar, S.; Filippakopoulos, P.; Picaud, S.; Keates, T.; Felletar, I.; Ciulli, A.; Knapp, S.; Heightman, T. D., Bromodomain-peptide displacement assays for interactome mapping and inhibitor discovery. *Mol. BioSyst.* **2011**, *7*, 2899-2908.